Gradient drift instability in Hall plasma devices

IEPC-2013-175

Presented at the 33^{rd} International Electric Propulsion Conference,
The George Washington University, Washington, D.C., USA
October 6–10, 2013

W.Frias* and A.I. Smolyakov†
University of Saskatchewan , Saskatoon, SK, S7N 5E2, Canada
Y. Raitses‡ and I. D. Kaganovich§
Princeton Plasma Physics Laboratory, Princeton University, Princeton, NJ, 08543, USA

Hall plasma devices with electron $\mathbf{E} \times \mathbf{B}$ drift are subject to a class of long wavelength instabilities driven by the electron current and gradients of plasma parameters. In this paper we apply the revisited theory to some thruster configurations and compare the results with the predictions from the earlier theory [Esipchuk Y.V., Tilinin G.V., Sov. Phys. Techn. Physics 21, 417 (1976)]. The earlier work had used an additional assumption of constant ion flux ($n_0 v_{0i} = const$), which is not true for the typical profiles. The differences in prediction of various models are described here.

I. Introduction

Plasmas with $\mathbf{E} \times \mathbf{B}$ are characterized by a wide range of turbulent fluctuations. These fluctuations are thought to be responsible for the observed anomalous transport across the magnetic field[1–3] and other nonlinear phenomena such as coherent rotating structures (spoke).[4,5] In order to understand the mechanisms responsible for the anomalous transport, a study of the instabilities in Hall plasma devices is needed. In an earlier work,[6] the authors of this paper reviewed the theory of linear instabilities due to gradients of density and magnetic field, starting with earlier derivations[7,8] and shown that the effects of plasma compressibility were not fully included in previous theory and quantitative corrections are required for accurate description of the growth rate and real part of frequency. The model was also extended to include effects of temperature gradients by developing a three fluid theory that takes into account the equation for the electron energy.

In this article we will apply the result of the theory presented in Ref. 6 to some realistic parameters observed in Hall thrusters. We use experimental data for a 2 kW Hall thruster from the Hall Thruster experiment (HTX) at Princeton Plasma Physics Laboratory (PPPL),[9,10] numerically simulated profiles for the plasma density, potential, electron temperature and magnetic field obtained using the numerical code HPHall-2 for the SPT-100 thruster[11] as well as data from the CAMILA Hall thruster at the Technion-Israel Institute of Technology.[12] We will focus on how plasma parameters, namely the equilibrium $\mathbf{E} \times \mathbf{B}$ drift, gradients of plasma density, temperature and magnetic field affect the characteristics, excitation conditions and localization of the linear instabilities.

In the previous work by Esipchuk and Tilinin,[7] the density gradient was absent as an independent parameter controlling the instability because they assumed absence of ionization and neglected the ion flux divergence. Experimental data show that these assumptions are not valid, and, as a result, their theory is inapplicable in such regions. Our theory retains the plasma density gradient as an independent parameter, which is critically important for valid predictions of the stability of Hall thrusters. We compare the predictions based on Refs.[7] and 6.

II. Gradient Drift Instability

Complete analysis of the gradient drift instability is presented in Ref. 6. It is done for a simplified geometry of a coaxial Hall thruster with the equilibrium electric field $\mathbf{E}_0 = E_0 \widehat{\mathbf{x}}$ in the axial direction, and with inhomogeneous

*Graduate Student, Department of Physics & Engineering Physics, winston.frias@usask.ca .
†Professor Department of Physics & Engineering Physics, andrei.smolyakov@usask.ca .
‡Research Physicist, Princeton Plasma Physics laboratory (PPPL), yraitses@pppl.gov.
§Research Physicist, Princeton Plasma Physics laboratory (PPPL), ikaganov@pppl.gov.

density $n = n_0(x)$ and electron temperature $T = T_e(x)$. Locally, Cartesian coordinates (x, y, z) are introduced with the z coordinate in the radial direction and y in the symmetrical azimuthal direction. The magnetic field is assumed to be predominantly in the radial direction, $\mathbf{B} = B_0(x)\,\hat{\mathbf{z}}$. Assuming constant electron temperature, the dispersion relation for the two field model is given by[6]

$$\omega - k_x v_0 = \frac{1}{2}\frac{k_\perp^2 c_s^2}{\omega_* - \omega_D} \pm \frac{1}{2}\frac{k_\perp^2 c_s^2}{\omega_* - \omega_D}\sqrt{1 + 4\frac{k_x v_0}{k_\perp^2 c_s^2}(\omega_* - \omega_D) - 4\frac{k_y^2}{k_\perp^2}\rho_s^2\Delta}, \tag{1}$$

where v_0 is the ion drift velocity in the axial $\hat{\mathbf{x}}$ direction, $\omega_D = -2k_y cT_e/(eB_0L_B)$ and $\omega_* = -k_y cT_e/(eB_0L_N)$, are the magnetic and density gradient drift frequencies, $1/L_B = \partial \ln B_0/\partial x$ and $1/L_N = \partial \ln n_0/\partial x$, are the magnetic field and density characteristic variation lengths, $\Delta = (\partial \ln B_0^2/\partial x + eE_0/T_e)(\partial \ln(n_0/B_0^2)/\partial x)$, $\rho_s^2 = T_e m_i c^2/e^2 B_0^2$. The effects of the temperature gradient are fully included in Ref. 6.

From Eq. (1), the conditions for instability in the two field model, assuming purely azimuthal propagation can be written as:

$$\left(\frac{\partial}{\partial x}\ln B_0^2 + \frac{eE_0}{T_e}\right)\frac{\partial}{\partial x}\ln\left(\frac{n_0}{B_0^2}\right) > \frac{1}{4\rho_s^2}. \tag{2}$$

The long wavelength instabilities described by Eq. (1) have the equilibrium electron flow as the main driving source of the instability, which is triggered by the presence of the gradients of plasma density and magnetic field.

A very well known model for gradient drift instabilities is the one proposed by Morozov[13] and extended by Esipchuk and Tilinin.[7] This model includes the electron drift effects related to the plasma density gradient with the assumption that the plasma density gradient can be related to the electric potential gradient using the density conservation equation and assuming a ballistic ion acceleration. With these assumptions, the dispersion relation is given by[7]

$$(\omega - k_x v_{0i})^2 + \frac{k^2 v_{0i}^2}{k_y(u_0 - u_B)}\omega - \frac{k^2 v_{0i}^2}{k_y(u_0 - u_B)}k_y u_0 = 0, \tag{3}$$

where u_0 is the $E_0 \times B_0$ equilibrium drift velocity and $u_B = (v_{0i}^2/\Omega_{ci})(\partial/\partial x)\ln(n_0/B_0)$ is the magnetic drift velocity. Under the assumption that $u_0^2 >> v_{0i}^2$, Esipchuk and Tilinin gave the following conditions for instability[7] $(\partial/\partial x)\ln(n_0/B_0) > 0$ and $\partial B_0/\partial x > 0$. These conditions basically suggest that the instability cannot be present in regions of decreasing magnetic field, such as the plume of the thruster. The goal of this paper is compare the prediction of the instability based on Eqs. (1) and (3).

III. Stability Analysis

In this section we will solve the dispersion relation for each model using the plasma parameters obtained in three different experiments[9,10,12] and simulations.[11]

A. PPPL Hall Thruster Experiment (HTX)

The Princeton Plasma Physics Laboratory hosts a 2kW laboratory Hall thruster with a channel length of 46 mm, an outer diameter of 123 mm and a width of 15 mm. Measurements of the plasma profiles this thruster are presented in Ref. 9. The measurements correspond mainly to the region from $x = -0.8$ cm to $x = 8.0$ cm (the exit plane is at x=0). The profiles are shown in Fig. 1. As can be seen, the magnetic and electric fields peak close to the exit plane and both density and temperature are decaying, except for a region close to x=0.

The solution to the two field model and to the Morozov dispersion relations for the measured profiles are shown in Fig. 2.

The instability predicted by the two-field model is concentrated in two narrow regions (see Fig. 2) from x=1.22 cm to x=1.82 cm and from x=5.54 cm to x= 6.22 cm. For the instability to occur, the condition Eq. (2) has to be true. In the region x<1.22 cm, we have $1/L_N - 2/L_B < 0$ but the first one, $eE_0/T_e + 2/L_B$ is positive, resulting in this region being stable. The region between x=1.22 cm and x=1.82 cm is characterized by $1/L_N - 2/L_B > 0$, and $eE_0/T_e + 2/L_B > 0$, resulting in instability. In this region, the magnetic field gradient is negative and the electric field satisfies the following inequality

$$E_0 > \frac{T_e}{e}\left|\frac{2}{L_B}\right|. \tag{4}$$

This last condition suggests that in the plume region, when the magnetic field gradient length L_B is larger than twice the density gradient length L_N, the instability will occur if the electric field is larger than a certain threshold value as

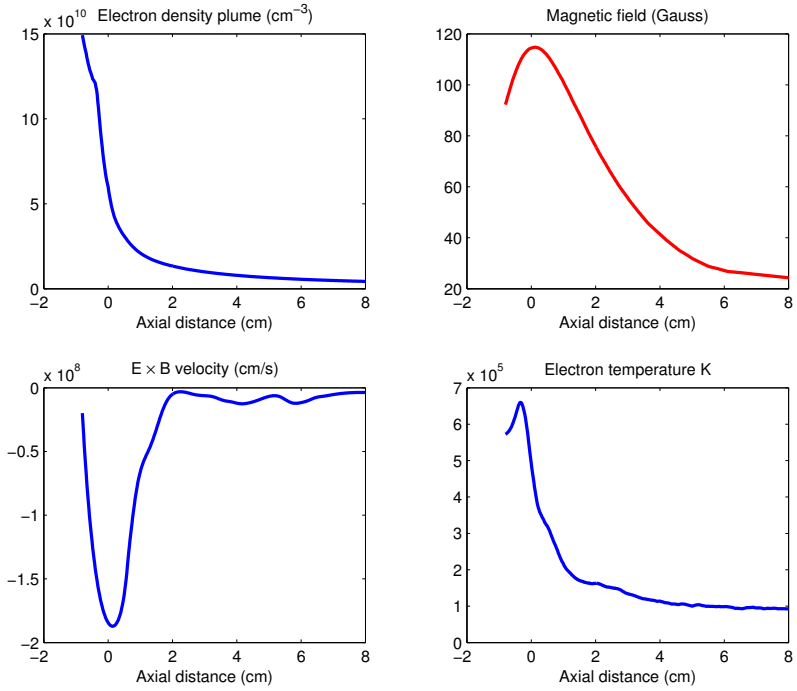

Figure 1: Experimental profiles of the plasma density, magnetic field, electron equilibrium drift velocity, u_0, and electron temperature for the HTX thruster.[9] The exit plane is at x=0.

expressed by Eq. (4). In the region between x=1.82 cm and x=5.54 cm, $1/L_N - 2/L_B > 0$ but the electric field is smaller than the threshold value From x=5.54 cm to x=6.22 cm, the electric field is larger than the threshold value and the instability reappears. For x> 6.22 cm, $1/L_N - 2/L_B < 0$ and the region becomes stable.

The real part of the frequency predicted by the two field model is negative, since it depends on the sign of $1/L_N - 2/L_B$. This way, the azimuthal phase velocity is in the same direction as the equilibrium drift velocity u_0 (see Fig. 1).

The Morozov instability is strongest in a small region close to the channel exit. The maximum of the growth rate in this region is 70 KHz and the frequency, which is negative, reaches a maximum absolute value of 0.033 KHz. This region was predicted to be stable by the two field model. Also in the plume region there are some unstable pockets whose growth rates do not exceed 10 KHz. These instabilities are most likely associated to the calculation of the gradient lengths. The very small value of the growth rate in the plume region is in agreement with the predictions from Eq. (3), in which the instabilities die out in regions of negative gradients of density and magnetic field.[7]

B. SPT-100 Thruster Simulations

Plasma parameters in the discharge chamber and near plume region the of SPT-100 Hall thruster were obtained by Hoffer with the HPHall-2 code[14,15] as reported in Ref. 11. These plasma profiles are in good agreement with the available experimental data for the SPT-100 thruster and can be seen in in Fig. 3.

The plasma density and magnetic field increase in the channel region, with the magnetic field reaching a maximum at the channel exit and the density peaking at a distance of 1.5 cm from the anode. In the region between x=1.5 cm to x=2.5 cm, the density and magnetic field gradient lengths are of opposite signs, with the density gradient length being negative and the magnetic field gradient length being positive. No instability is expected in this region. The electron temperature and the electric field also reach their maximum values at the exit plane.

The growth rate and frequency obtained for the two field model and the Morozov dispersion relation are shown in Fig. 4.

For the profiles shown in Fig. 3, there is an unstable region inside the channel from x=0.03 cm to x=0.8 cm, that is close to the anode. This instability growth rate is in the 100-450 KHz range, the growth rate being larger when

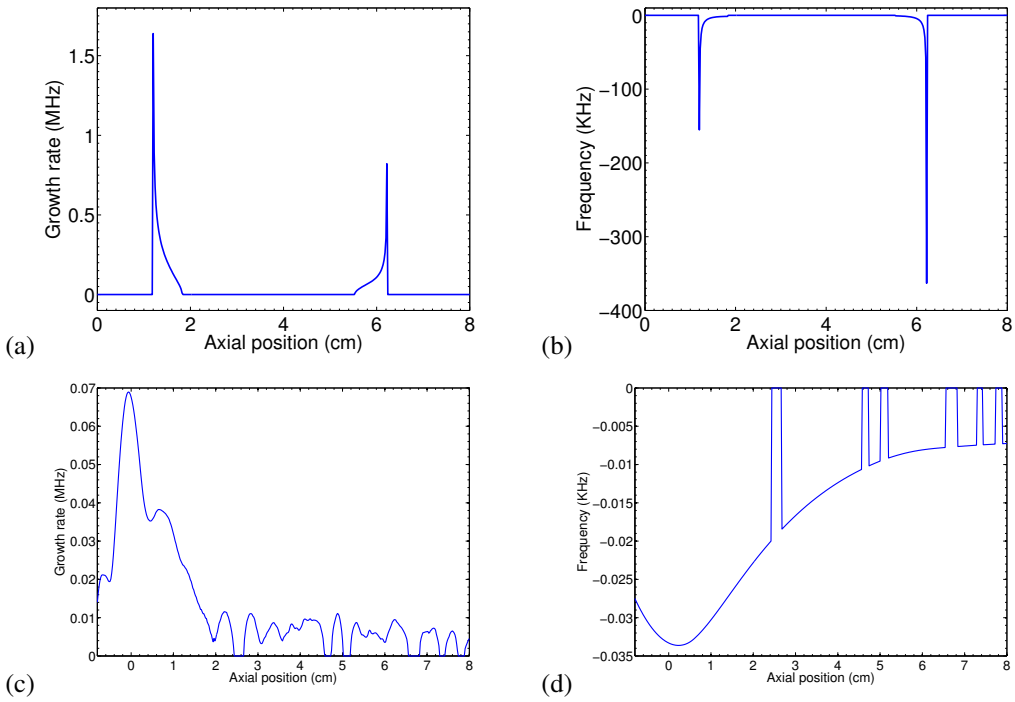

Figure 2: Growth rate and frequency of the instabilities in the HTX thruster[9] as a function of axial distance as predicted by the two-field model (a and b) and by the Morozov model (c and d). The exit plane is at x=0.

the temperature gradients are not considered. In this region, both $1/L_N - 2/L_B$ and the factor $eE_0/T_e + 2/L_B$ are positive, resulting in instability. For x between 0.8 cm and 2.5 cm (exit plane), the density and magnetic field gradient lengths are of opposite signs. In this region, $1/L_N - 2/L_B$ changes sign, becoming positive, while at the same time $eE_0/T_e + 2/L_B$ remains positive, and the region is stable. In the region from x=2.5 cm to x=3.0 cm, $1/L_N - 2/L_B < 0$, but the electric field is larger than the threshold value $2T_e/e|L_B|$ resulting in stability.

In the region between x=3.0 cm and x=3.2 cm the unstable modes propagate with positive frequency. In this region, the electric field is smaller than the threshold electric field, $E < E_{thr}$ and the instability criterion is simply determined by the sign of the factor $1/L_N - 2/L_B$; the mode is unstable for $1/L_N - 2/L_B < 0$. The sign of the real part of the frequency is only determined by the sign of $1/L_N - 2/L_B$, so that the unstable modes propagate with positive frequency, in the direction opposite to $\mathbf{E}_0 \times \mathbf{B}_0$. Generally, two field model predicts that the direction of propagation of unstable modes is directly linked to the sign of the quantity $(\mathbf{E}_0 - \mathbf{E}_{thr}) \times \mathbf{B}_0$, thus negative (in the direction of $\mathbf{E}_0 \times \mathbf{B}_0$ flow) for $E_0 > E_{thr}$, and positive when $E_0 < E_{thr}$. Some experiments with $\mathbf{E}_0 \times \mathbf{B}_0$ plasmas do show the presence of fluctuations with rotation in the direction opposite to $\mathbf{E}_0 \times \mathbf{B}_0$ drift.[16]

The instability predicted by Eq. (3) is present mainly in the channel region of the thruster, different to the one predicted by the two field model in Eq. (1), that is concentrated mainly in the near anode region. Its peak in the channel region is located at the point where the plasma density reaches its maximum value and reaches a value of close to 300 KHz. After that, the growth rate decreases with distance. It features a peak outside of the channel region due to the resonance of u_0 and u_B. This resonance explains the peak of the real value of the frequency present at x=2.9 cm with an absolute value of 30 KHz, that can be seen in Figs. 4c and Figs. 4d.

C. CAMILA Thruster Simulations

The coaxial magnetoisolated longitudinal anode thruster (CAMILA) was developed at the Technion's Asher Space Research Institute is an effort to adapt Hall thruster technology to low power regimes.[12] This thruster is characterized by having a longitudinal magnetic field inside the anode cavity that reduces the electron mobility in the radial direction. A radial electric field is created in the direction towards the center of the channel. Two configurations are currently under development, simplified CAMILA, without anode coils and full CAMILA, with anode coils. In the following

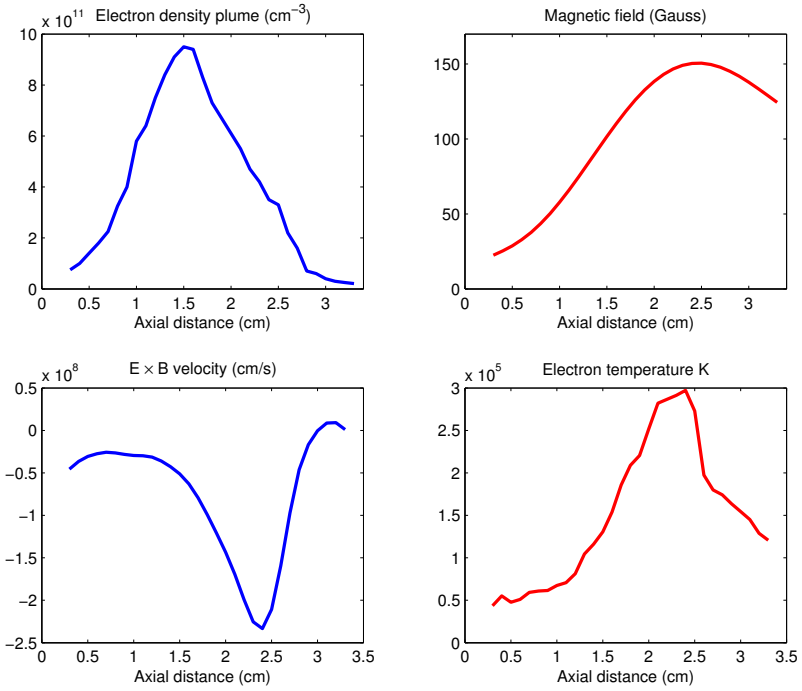

Figure 3: Plasma density, magnetic field, electron equilibrium drift velocity, u_0, and electron temperature profiles in SPT-100 Hall thruster obtained from HPHall-2 simulations as shown in Fig. 10 from Ref. 11. The exit plane is at x=2.5 cm.

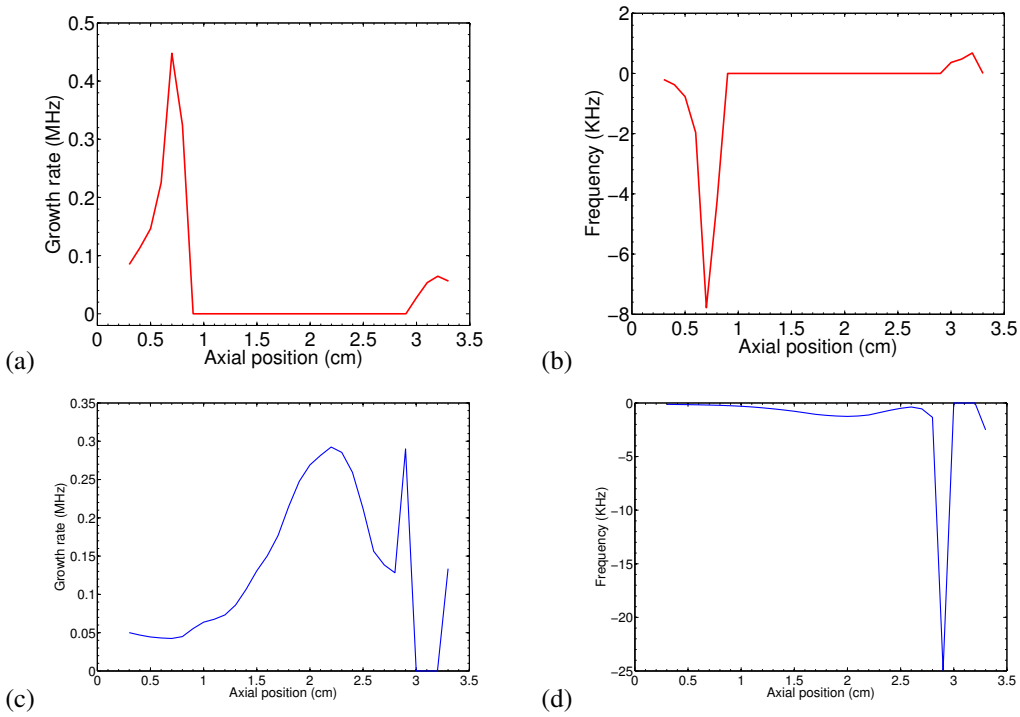

Figure 4: Growth rate and frequency of the instabilities in a SPT-100 thruster[11] as a function of axial distance to the anode as predicted by the two-field model (a and b) and Morozov model (c and d). The exit plane is at x=2.5 cm.

we will refer to the simplified version of the thruster. A more detailed description of the CAMILA concept can be found in Ref. 12 and references therein. The plasma parameter profiles for the CAMILA thruster are shown in Fig. 5.[12]

The magnetic field is positive and increasing with distance in the channel region, reaching its maximum value at the channel exit, located at x=0, which results in a positive magnetic field gradient length $L_B = (\partial \ln B/\partial x)^{-1} > 0$ inside the channel, except for the region from x=-3.0 to -2.9 cm. The plasma density reaches its maximum value at a distance of x=-0.8 cm from the exit plane, decreasing afterwards, resulting in a positive density gradient length $L_N = (\partial \ln n/\partial x)^{-1} > 0$ from x=-3.0 cm to x=-0.8 cm and in a negative density gradient length $L_N = (\partial \ln n/\partial x)^{-1} < 0$ from x=-0.8 cm up to the exit plane. The regions between x= -3.0 and -2.9 and x=-0.8 cm to x=0 have density and magnetic field gradient lengths of opposite signs. The instability is not present in this region. The electron temperature reaches its maximum value close to the exit plane, at x=-0.4 cm, resulting in a positive temperature gradient length $L_T = (\partial \ln T_e/\partial x)^{-1} > 0$ for most of the region under consideration. Similarly to the magnetic field and electron temperature, the electric field reaches its maximum value at the exit plane.

One peculiarity of the CAMILA magnetic field is the additional presence of an axial component. This way, the magnetic field B_0 in dispersion relation, Eqs. (1) refers to the magnitude of the field. The growth rate and frequencies of the unstable modes calculated from the two field model and the Morozov dispersion relation are shown in Fig. 6.

For the profiles shown in Fig. 5, there are two unstable regions close to the anode. The first of these regions corresponds to the interval from x=-2.8 cm to x=-2.5 cm, where the maximum value for the growth rate is 280 KHz at x=-2.5 cm. The second unstable region corresponds to the interval from x=-2.0 cm to x=-1.9 cm, where the peak of the growth rate is 367 KHz at a position x=-2.0 cm. These two unstable regions have $1/L_N - 2/L_B 0$ and $eE_0/T_e + 2/L_B$ positive, resulting in the appearance of the instability. For x between -1.9 cm and x=0, the plasma density decreases while the magnetic field is still increasing. Here, the factor $1/L_N - 2/L_B$ becomes negative while $eE_0/T_e + 2/L_B$ remains positive, resulting in the disappearance of the instability. In the unstable regions, since $1/L_N - 2/L_B > 0$, the real part of the frequency is negative.

The dispersion relation from Eq. (3) predicts instability throughout the channel region, similar to the case with the SPT-100 thruster. This region is characterized by a valley in the gradient of magnetic field. The growth rate for the CAMILA thruster is notably higher than the one predicted for the SPT-100 thruster and one order of magnitude higher

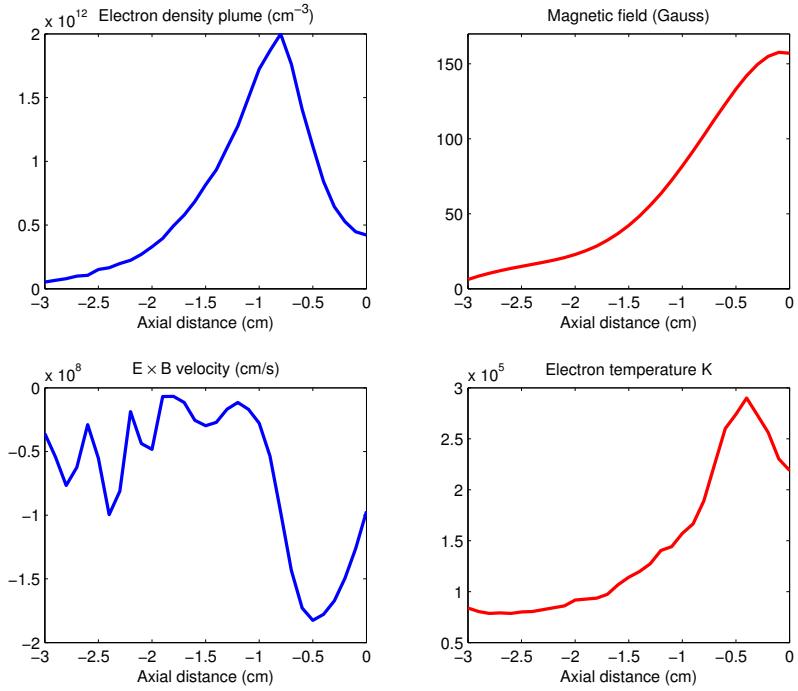

Figure 5: Plasma density, magnetic field, electron equilibrium drift velocity, u_0, and electron temperature profiles in CAMILA Hall thruster from Ref. 12. The exit plane is at x=0.

than the predicted by the two field model. The similar is true for the frequency.

IV. Summary

In this work, we have presented a comparison of the results obtained from the study of the gradient drifts instabilities using our two field model[6,17] and the gradient drift model proposed by Morozov.[7,13] The dispersion relation model predicts instability in a wider region of the thruster. This instability is present throughout the channel region of the thruster, whereas the two field model predicts that the instability is concentrated mainly in the near anode region of the thruster and is absent from the acceleration region, where the instability from Eq. (3) is at its strongest. The instability is similarly enhanced by a resonance of the $E_0 \times B_0$ electron drift velocity and the magnetic drift velocity, u_B. In our two field model, the resonance is between the density and magnetic gradient drift velocities. The model proposed in Ref. 7 does not include the density gradient in an explicit way, but takes it into account via the $E_0 \times B_0$ electron drift velocity. Also the gradient drift velocity is introduced assuming that for the unperturbed plasma $n_0(x)v_{0i}(x) = const$,[7,13] assumption that is generally not true for the profiles presented above (see Ref. 17).

V. Acknowledgements

The authors thank Dr. Nathaniel J. Fisch for helpful discussions, Dr. Richard Hofer for allowing the use of the data from the HPHall-2 simulations and Drs. Igal Kronhaus and Alexander Kapulkin for providing the data for the CAMILA Hall thruster. This work was sponsored by the Natural Sciences and Engineering Research Council of Canada and partially supported by the Air Force Office of Scientific Research and the US Department of Energy.

References

[1] Keidar, M. and Beilis, I., "Electron transport phenomena in plasma devices with E x B drift," *Ieee Transactions on Plasma Science*, Vol. 34, No. 3, 2006, pp. 804–814.

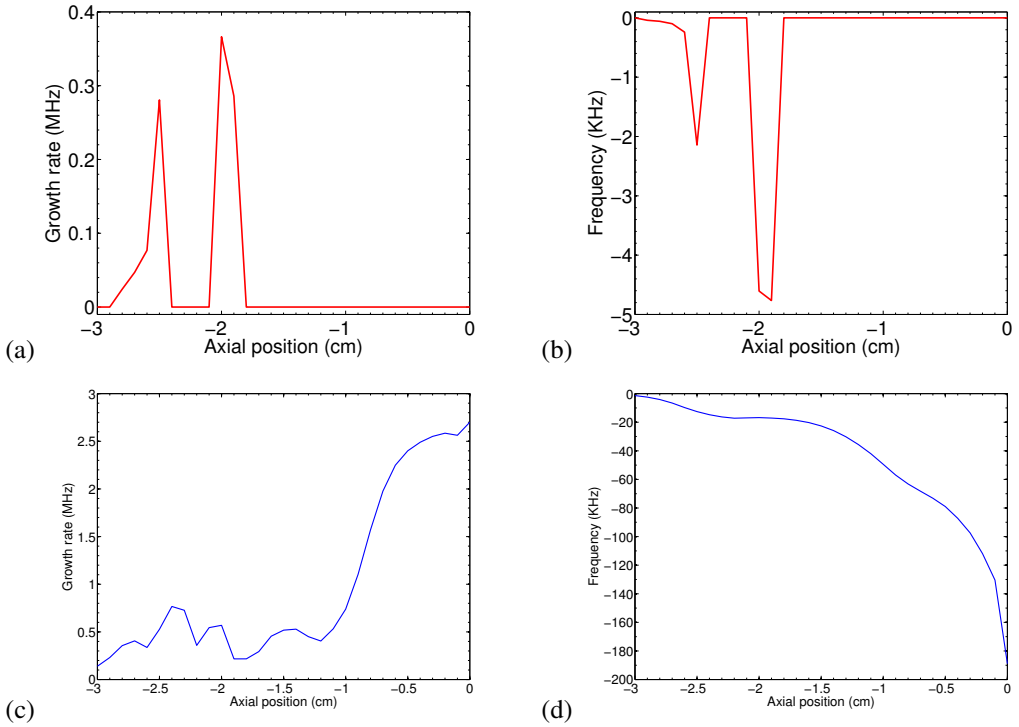

Figure 6: Growth rate and frequency of the instabilities in the CAMILA thruster[12] as a function of axial distance to the anode as predicted by the two-field model (a and b) and the Morozov model (c and d). The exit plane is at x=0.

[2]Hagelaar, G. J. M., Bareilles, J., Garrigues, L., and Boeuf, J. P., "Role of anomalous electron transport in a stationary plasma thruster simulation," *Journal of Applied Physics*, Vol. 93, No. 1, 2003, pp. 67–75.

[3]Adam, J. C., Boeuf, J. P., Dubuit, N., Dudeck, M., Garrigues, L., Gresillon, D., Heron, A., Hagelaar, G. J. M., Kulaev, V., Lemoine, N., Mazouffre, S., Luna, J. P., Pisarev, V., and Tsikata, S., "Physics, simulation and diagnostics of Hall effect thrusters," *Plasma Physics and Controlled Fusion*, Vol. 50, No. 12, 2008.

[4]Ellison, C. L., Raitses, Y., and Fisch, N. J., "Cross-field electron transport induced by a rotating spoke in a cylindrical Hall thruster," *Physics of Plasmas*, Vol. 19, No. 1, 2012, pp. 013503.

[5]Griswold, M. E., Ellison, C. L., Raitses, Y., and Fisch, N. J., "Feedback control of an azimuthal oscillation in the E x B discharge of Hall thrusters," *Physics of Plasmas*, Vol. 19, No. 5, 2012.

[6]Frias, W., Smolyakov, A. I., Kaganovich, I. D., and Raitses, Y., "Long wavelength gradient drift instability in Hall plasma devices. I. Fluid theory," *Physics of Plasmas*, Vol. 19, No. 7, 2012, pp. 072112.

[7]Esipchuk, Y. V. and Tilinin, G. N., "Drift Iinstability in a Hall-current plasma accelerator," *Sov. Phys. Tech. Phys.*, Vol. 21, No. 4, 1976, pp. 417–423.

[8]Kapulkin, A. and Guelman, M. M., "Low-Frequency Instability in Near-Anode Region of Hall Thruster," *Ieee Transactions on Plasma Science*, Vol. 36, No. 5, 2008, pp. 2082–2087.

[9]Raitses, Y., Staack, D., Keidar, M., and Fisch, N., "Electron-wall interaction in Hall thrusters," *Physics of Plasmas*, Vol. 12, No. 5, 2005, pp. 057104.

[10]Dorf, L., Raitses, Y., and Fisch, N. J., "Effect of magnetic field profile on the anode fall in a Hall-effect thruster discharge," *Physics of Plasmas*, Vol. 13, No. 5, 2006, pp. 057104.

[11]Hofer, R., Mikellides, I., Katz, I., and Goebel, D., "Wall Sheath and Electron Mobility Modeling in Hybrid-PIC Hall Thruster Simulations," *43rd AIAA/ASME/SAE/ASEE Joint Propulsion Conference & Exhibit*, 2007, pp. AIAA 2007–5267.

[12]Kronhaus, I., Kapulkin, A., Balabanov, V., Rubanovich, M., Guelman, M., and Natan, B., "Investigation of physical processes in CAMILA Hall thruster using electrical probes," *Journal of Physics D: Applied Physics*, Vol. 45, No. 17, 2012, pp. 175203.

[13]Morozov, A. I., Esipchuk, Y. V., Kapulkin, A., Nevrovskii, V., and Smirnov, V. A., "Effect of the magnetic field on a closed-electron-drift accelerator," *Sov. Phys. Tech. Phys.*, Vol. 17, No. 3, 1972, pp. 482–487.

[14]Parra, F., Ahedo, E., Fife, J., and Martinez-Sanchez, M., "A Two-Dimensional Hybrid Model of the Hall Thruster Discharge," *J. Appl. Phys.*, Vol. 100, No. 3, 2006, pp. 023304.

[15]Fife, J., "Hybrid-PIC Modeling and Electrostatic Probe Survey of Hall Thruster," *PhD Thesis, Aeronautics and Astronautics, Massachussets Institute of Technology.*, 1998.

[16]Ito, T. and Cappelli, M. A., "High Speed Images of Drift Waves and Turbulence in Magnetized Microplasmas," *Plasma Science, IEEE Transactions on*, Vol. 36, No. 4, 2008, pp. 1228–1229.

[17]Frias, W., Smolyakov, A. I., Kaganovich, I. D., and Raitses, Y., "Long wavelength gradient drift instability in Hall plasma devices. II. Applications," *Physics of Plasmas*, Vol. 20, No. 5, 2013, pp. 052108.